# Identification and biophysical assessment of the molecular recognition mechanisms between the human hemopoietic cell kinase Src homology domain 3 and ALG-2-interacting protein X

Xiaoli Shi, Sandrine Opi, Adrien Lugari, Audrey Restouin, Thibault Coursindel, Isabelle Parrot, Javier Perez, Eric Madore, Pascale Zimmermann, Jacques Corbeil, et al.

# Identification and biophysical assessment of the molecular recognition mechanisms between the human hemopoietic cell kinase Src homology domain 3 and ALG-2-interacting protein X

Xiaoli Shi[*†‡1], Sandrine Opi[§1], Adrien Lugari[‡1], Audrey Restouin[§], Thibault Coursindel[‖], Isabelle Parrot[‖], Javier Perez[¶], Eric Madore[**], Pascale Zimmermann[††], Jacques Corbeil[**], Mingdong Huang[*], Stefan T. Arold[‡‡§§], Yves Collette[§] and Xavier Morelli[‡2]

[*]State Key Laboratory of Structural Chemistry, Fujian Institute of Research on the Structure of Matter, Chinese Academy of Sciences, 155 Yang Qiao Xi Lu, Fuzhou, Fujian 350002, China,
[†]Graduate School of the Chinese Academy of Sciences, Beijing 10039, China,
[‡]IMR Laboratory (UPR 3243), Centre National de la Recherche Scientifique–Institut de Microbiologie de la Méditerranée (IMM) & Aix-Marseille Universités, 31 Chemin Joseph Aiguier, 13402 Marseille Cedex 20, France
[§]INSERM U891, Centre de Recherche en Cancérologie de Marseille, 13009 Marseille, France; Institut Paoli Calmettes, 13009 Marseille, France; Université de la Méditerranée, 13007 Marseille, France
[‖]Institut des Biomolécules Max Mousseron (IBMM), UMR 5247 CNRS–Université Montpellier 1–Université Montpellier 2, cc17-03, Place Eugène Bataillon, 34095 Montpellier Cedex 5, France,
[¶]Synchrotron SOLEIL–SWING, L'Orme des Merisiers, BP48 Saint-Aubin, 91192 Gif-sur-Yvette Cedex, France,
[**]Centre de Recherche en Infectiologie- Centre Hospitalier Universitaire de Québec, Pavillon CHUL, 2705 Laurier Blvd., Québec, QC, Canada G1V 4G2,
[††]Department of Human Genetics, Katholieke Universiteit Leuven, Herestraat 49 Box 602, 3000 Leuven, Belgium,
[‡‡]INSERM, Unité 554, Montpellier, France and Université de Montpellier, CNRS, UMR 5048, Centre de Biochimie Structurale, 29 rue de Navacelles, 34090 Montpellier cedex, France
[§§]Department of Biochemistry and Molecular Biology, Unit 1000, The University of Texas MD Anderson Cancer Center, 1515 Holcombe Blvd., Houston, TX 77030-4009, USA

[1] These authors contributed equally to this work as first authors.
[2] Correspondence should be addressed to XM (morelli@ifr88.cnrs-mrs.fr).

Running Title: Molecular Recognition Mechanisms between Hck-SH3 and Alix

Abbreviations used: ALG-2, apoptosis-linked-gene-2; Alix, ALG-2 interacting protein X; DMF, *N*,*N*-dimethylformamide; DTT, dithiothreitol; EGFP, enhanced green fluorescent protein; EOM, ensemble optimization method; GFP, green fluorescent protein; GST, glutathione *S*-transferase; Hck, hemopoietic cell kinase; HEK-293, human embryonic kidney 293; HRP, horseradish peroxidase; HSQC, heteronuclear single quantum coherence; IPTG, isopropyl β-D-thiogalactopyranoside; ITC, isothermal titration calorimetry; NTA, nitrilotriacetic acid; PDB, Protein Data Bank; PPII, polyproline type II; PRR, proline-rich region; SAXS, small-angle X-ray scattering; SFKs, Src family of nonreceptor protein tyrosine kinases; SH, Src homology; SUMO, small ubiquitin-related modifier; TFA, 2,2,2-trifluoroacetic acid.

**SYNOPSIS**

Src family kinases (SFKs) are central regulators of many signaling pathways. Their functions are tightly regulated through SH (Src homology) domain-mediated protein–protein interactions. A yeast two-hybrid screen using SH3 domains as bait identified Alix (ALG-2 [apoptosis-linked gene 2]-interacting protein X) as a novel Hck (hemopoietic cell kinase) SH3 domain interactor. The Alix–Hck-SH3 interaction was confirmed *in vitro* by a GST (glutathione *S*-transferase) pull-down assay and in intact cells by a mammalian two-hybrid assay. Furthermore, the interaction was demonstrated to be biologically relevant *in cellulo*. Through biophysical experiments, we then identified the PRR (proline-rich region) motif of Alix that binds Hck-SH3 with a dissociation constant of 34.5 μM. Heteronuclear NMR spectroscopy experiments was used to map Hck-SH3 residues that interact with the $ALIX_{V+PRR}$ construct or with the minimum identified interacting motif. Finally, small-angle X-ray scattering (SAXS) analysis showed that the N-terminal PRR of Alix is unfolded, at least before Hck-SH3 recognition. Our results indicate that residues outside the canonical PxxP motif of Alix enhance its affinity and selectivity toward Hck-SH3. The structural framework of the Hck–Alix interaction demonstrated here will help in clarifying how Hck and Alix assist during virus budding and cell surface receptor regulation.



Keywords: Src family kinase, SH3 domains, Alix, protein–protein interaction, Hck

## INTRODUCTION

SFKs (the Src family of nonreceptor protein tyrosine kinases) consist of nine members: Src, Blk, Fgr, Fyn, Hck, Lyn, Lck, Yes, and Frk. Whereas Fyn, Src, and Yes are ubiquitously expressed and mediate diverse signaling pathways, the other SFKs show a more restricted tissue distribution with more specific biochemical tasks, such as Hck (hemopoietic cell kinase) in myeloid cells. SFKs play crucial roles in a variety of cellular processes, including cell cycle control, adhesion, motility, proliferation, and differentiation [1]. Extensive studies have indicated that the complexity of the functional roles of SFKs derives mainly from their ability to communicate with a large number of upstream receptors and downstream effectors which vary by cell type and are largely dependent on the structural organization of the SFKs [2]. Tight regulation of the structure and activity of SFKs is essential for normal cellular function as abnormally elevated activity of SFKs is a common feature of several forms of cancer and infectious diseases [3,4]. SFKs have therefore developed diverse mechanisms of autoregulation, based on inhibitory intramolecular interactions between their different domains.

From the N-terminus to the C-terminus, SFKs contain: a myristoyl group (SH [Src homology] 4) which is required for membrane attachment; a unique domain, which may impart distinct localization properties to the individual family members; an SH3 domain, which typically binds left-handed PPII (polyproline type II) sequence motifs; an SH2 domain, which binds to phosphotyrosine-containing proteins; an SH2–kinase linker; a protein tyrosine kinase domain (SH1); and a C-terminal regulatory segment. The protein–protein interaction modules (especially the SH2 and SH3 domains) in SFKs have dual roles. First, their interactions with intramolecular binding motifs promote an “assembled” and inactive state of the SFKs [5,6]. Second, intermolecular recognition of the SH2 and SH3 domains by ligand proteins activates the SFKs and targets them to the proper intracellular sites and substrates [5–10]. The identification and characterization of binding partners that regulate the kinase activity and/or constitute downstream signaling molecules is therefore important to understand the function and dysfunction of these SFKs.

Alix (ALG-2-interacting protein X) has previously been identified as a binding partner of various proteins (i.e. CHMP4, Gag, TSG101, and endophilins) and has been demonstrated to be implicated in many diverse cellular processes, both normal and pathogenic, including regulation of apoptosis, cytoskeletal dynamics, receptor cell surface internalization, endosomal sorting processes, and virus budding from infected cell membranes [11–16]. Recently, crystal structures revealed that human Alix is composed of three domains: the N-terminal Bro1 domain (residues 1–358), a central V domain (residues 362–702), and a C-terminal PRR (proline-rich region; residues 703–868) (Figure 1) [17]. The Bro 1 domain and the V domain have been described to interact with cellular proteins and viral composition respectively, and to facilitate virus budding [18,19]. In contrast, the C-terminal PRR was found to be critical for the interaction of Alix with most proteins that connect Alix to cellular processes; one example is the association of Alix with SH3 domains [20]. In this present work, we identified Alix as a novel Hck SH3-binding protein by using a yeast two-hybrid screen with the SH3 domains of SFKs. We demonstrate that Alix binds to and activates Hck, delineate the proline-rich motif part of the Alix PRR that binds to Hck, provide a structural analysis of the molecular

recognition mechanisms of Alix and Hck, and discuss a model of the functional repercussions of Hck binding to Alix during virus budding and regulation of cell surface receptors.

## EXPERIMENTAL

### Cell culture and transfection

HEK (human embryonic kidney)-293 cells were propagated in Dulbecco's modified Eagle's medium containing 10% fetal bovine serum at 37°C in a humidified 5% $CO_2$ atmosphere. For transfection, HEK-293 cells were grown in 6-well plates to about 70% confluence. The cells were transfected using jetPEI (Polyplus Transfection), following the manufacturer's recommendations. A total of 1 μg of plasmid DNA per well (1 μg/5 × $10^5$ cells) was used. Total amounts of transfected DNA were kept constant in all samples of any given experiment by adding empty-vector DNA (pXM) as appropriate. Cells were harvested at 48 h post-transfection. The human Hck plasmid construct was described previously [21], a full-length Alix sequence was subcloned into pEGFP-C2 plasmid (Clontech), and a full-length HIV-1 Nef sequence was subcloned into pEGFP-N3 plasmid (Clontech).

For immunoblot analysis of intracellular proteins, whole-cell lysates were prepared as follows. The cells were washed once with PBS and resuspended for 10 min at 4°C in lysis buffer (300 mM NaCl, 40 mM Hepes, 1 mM dithiothreitol [DTT], 0.1 mM $NaVO_4$, 1 mM NaF, protease inhibitor cocktail [Sigma-Aldrich], and 6 mM octyl-β-D-glucopyranoside, supplemented with 1% Triton X-100. Residual insoluble material was removed by centrifugation (10 min, 13,000 rpm, in an Eppendorf minifuge). Cell lysates were subjected to 10% SDS-PAGE; proteins were transferred to PVDF membranes and reacted with appropriate antibodies as described below. Membranes were then incubated with HRP (horseradish peroxidase)-conjugated secondary antibodies (Amersham Biosciences) and visualized by enhanced chemiluminescence (Amersham Biosciences).

### DNA construction and protein expression

The Alix cDNA spanning from the V domain to the PRR was amplified using a human fetal liver library as a template. A sticky-end PCR strategy was applied against the Alix cDNA to obtain recombinant genes encoding $ALIX_V$ (residues 362–702) and $ALIX_{V+PRR}$ (residues 362–760), respectively. The PCR products comprised two universal cloning sites (the 5′-*NdeI* and 3′-*BamHI* restriction sites) and could therefore be directionally subcloned into the modified pET11d-SUMOstar expression vector using the two restriction enzymes. The constructs were confirmed by DNA sequencing and expressed in *Escherichia coli* BL21 (DE3) cells with their N-terminal His6-Smt3 tag (designated as the SUMO [small ubiquitin-related modifier] tag), which can be removed by SUMO protease [22,23]. The cells were induced with 0.2 mM IPTG (isopropyl-β-D-thiogalactopyranoside) and then grown for 12 h at 16°C. Harvested cells were resuspended in lysis buffer (50 mM Tris-HCl pH8.0, 150 mM NaCl, 5 mM imidazole, 2 mM β-mercaptoethanol, and 0.1% *DNase I*). After the cells were broken up with a French press, the supernatant was mixed with 5 ml nickel–NTA (nitrilotriacetic acid) resin (QIAGEN) to capture the SUMO–Alix fusion protein. The protein was then washed with 30 ml of lysis buffer, and the nickel–NTA resin bound with the SUMO–Alix fusion protein was incubated with 0.5 mg of SUMO protease in cleavage buffer (50 mM Tris-HCl [pH 8.0], 150 mM NaCl, and 2 mM β-mercaptoethanol) for 1–2 h at 30°C to separate the Alix recombinant and the SUMO tag. The cleaved Alix recombinant was then released from the nickel–NTA column. The flow-through was collected, concentrated, and applied to a Superdex 75 column

(Amersham Biosciences) in 50 mM Tris-HCl (pH 8.0), 20 mM NaCl, and 2 mM β-mercaptoethanol.

To produce the recombinant Hck SH3 domain and simplify the procedure to purify it, cDNA encoding Hck-SH3 was amplified by PCR using the corresponding pGEX–Hck construct as a template [24]. The amplified DNA fragment was subcloned into an expression vector, pET-42a (Novagen), using the 5′-*NdeI* and 3′-*XhoI* restriction sites. The recombinant SH3 domain was expressed in *E. coli* BL21 (DE3) cells with its C-terminal $His_6$ tag. The cells were induced with IPTG (0.5 mM) and grown overnight at 20°C. Harvested cells were resuspended in lysis buffer and then French-pressed. The soluble fraction was loaded onto a nickel–NTA column and eluted by 50 mM Tris-HCl (pH 8.0), 150 mM NaCl, 500 mM imidazole, and 2 mM β-mercaptoethanol. The protein captured by the nickel–NTA column was concentrated and further purified by the Superdex 75 column. For pull-down assays, GST (glutathione *S*-transferase) and GST–SH3 recombinant proteins were expressed and purified as previously described [25].

**Immunoprecipitation and kinase assay**

For immunoprecipitation analysis of intracellular proteins, cell lysates were prepared as follows. Cells were washed once with PBS and lysed in 500 µl of lysis buffer (50 mM Hepes [pH 7.4], 100 mM NaCl, 50 mM NaF, 5 mM β–glycerophosphate, 2 mM EDTA, 2 mM EGTA, 1 mM $Na_3VO_4$, 1% Triton X-100, and protease inhibitor). The cell extracts were centrifuged at 13,000 *g* for 10 min, and the supernatant was incubated on a rotating wheel for 1 h at 4°C with anti-GFP (green fluorescent protein) mouse monoclonal antibody (Roche) or anti-Hck rabbit polyclonal antibody (sc-72, Santa Cruz Biotechnology) and coupled for 1 h at 4°C with protein G–Sepharose (Sigma-Aldrich). Immune complexes were washed three times with 50 mM Tris (pH 7.5), 15 mM EGTA, 100 mM NaCl, 0.1% Triton X-100, 0.5 mM $Na_3VO_4$, 10 mM NaF, 10 mM β–glycerophosphate, and protease inhibitor. Bound proteins were eluted from beads by heating in sample buffer for 5 min at 96°C and then analyzed by immunoblotting.

For the kinase assay, immune complexes were washed twice with tampon kinase (100 mM Hepes, 5 mM $MnCl_2$, 5 mM DTT, 5 mM $MgCl_2$, and 500 µM $Na_3VO_4$). Bound proteins were diluted in tampon kinase and incubated for 30 min at 30°C with varying amounts of ATP (0–10 µM) on a 96-well MaxiSorp plate previously coated with polyglutamine-tyrosine peptide (12.5 µg/well). After 30 min, the reaction was stopped by adding 50 mM EDTA, and the plate was washed twice with PBS 0.05% Tween. The fraction of phosphorylated substrate was visualized using a phosphotyrosine monoclonal antibody conjugated to HRP (A5964, Sigma-Aldrich) and an ensuing chromogenic substrate reaction.

**CheckMate assay**

The sequence from human $ALIX_{V+PRR}$ (residues 362–760) was amplified by PCR using Gateway technology (Invitrogen) and subcloned into a pACT plasmid using the CheckMate assay (Promega). pBIND plasmids coding for human wild-type Hck-SH3 or mutant Hck-SH3 were previously described [24]. We performed the CheckMate assay as recommended by the manufacturer. Briefly, $1–2 \times 10^5$ COS7 cells were spread in 100-mm dishes. After 24 h, vectors of pG5luc (300 ng) and pBC-KS plasmid carrier (200 ng) together with pACT or pACT–$ALIX_{V+PRR}$ and pBIND Hck-SH3 or pBIND mutant Hck-SH3 (100 ng) were transiently

co-transfected by lipofection using FuGENE 6 (Roche) according to the manufacturer's procedures. At 24 h post-transfection, luciferase activity was revealed using the Dual-Glo assay system (Promega) and measured with a Centro luminometer (Berthold Technologies).

**GST pull-down assay**

Purified $ALIX_{V+PRR}$ (residues 362–760) was pre-incubated at room temperature for 2 h in 500 µl of reaction buffer (25 mM Hepes [pH 7.8], 150 mM NaCl, 10 mM EDTA, and 1 mM EGTA, supplemented with 1% Triton X-100) with Sepharose-coupled recombinant GST or with GST Hck-SH3 (2 µg/reaction). After three washes with reaction buffer, complexes were resolved by 12% SDS-PAGE, stained with Coomassie Blue (Bio-Rad Laboratories) for 1 h, and destained in 40% methanol/10% acetic acid.

**Peptide synthesis**

***Automatic synthesis.*** The microwave synthesis was performed with the Liberty Microwave Peptide Synthesizer (CEM Corporation) that uses microwave energy at 2450 MHz to perform solid-phase peptide synthesis by following the fluorenylmethoxycarbonyl/*tert*-butyl strategy. Syntheses were conducted on a 0.1-mmol scale. Deprotections were performed with 20% piperidine in DMF (*N*,*N*-dimethylformamide). All coupling reactions were performed with 5 equivalents of O-Benzotriazole-*N,N,N',N'*-tetramethyl-uronium-hexafluoro-phosphate in DMF (0.5 M), 5 equivalents of amino acid in DMF (0.2 M), and 10 equivalents of *N*,*N*-Diisopropylethylamine in *N*-Methyl-2-pyrrolidone (2.0 M).

Each deprotection and coupling reaction was performed with microwave energy and nitrogen bubbling. Each microwave cycle was characterized by two deprotection steps, the first for 30 s and the second for 180 s. All coupling reactions were for 300 s. After the assembly was complete, the peptide resin was washed with $CH_2Cl_2$. Peptide cleavage from the resin and deprotection of the amino acid side chains were performed with TFA (2,2,2-Trifluoroacetic acid)/$CH_2Cl_2$ solution (9:1 v/v). In all cases, the cleavage was maintained for 1.5 h at 23°C. The resins were washed with TFA, and the filtrates were completely evaporated. The crude products were dissolved in $H_2O$/Acetonitrile and lyophilized.

***LC/MS purification.*** Samples were prepared in DMSO. The LC/MS autopurification system consisted of a binary pump (Waters 2525) and an injector/fraction collector (Waters 2676) coupled to a Waters Micromass ZQ mass spectrometer positive ion (electrospray ionization mode; $ESI^+$). All the purifications were carried out using a reversed-phase XBridge Prep $C_{18}$ 5-µm OBD 19 × 100 mm column (Waters) Eluent A was water/0.1% TFA; eluent B was acetonitrile/0.1% TFA. A flow rate of 20 ml/min and a gradient of 10–30% B over 10 min were used. Positive-ion electrospray mass spectra were acquired at a solvent flow rate of 204 µl/min. Nitrogen was used for both the nebulizing gas and the drying gas. The data were obtained in the scan mode from *m*/*z* 100 to 1000 in 0.1-s intervals; 10 scans were summed to obtain the final spectrum. The collection control trigger was set on singly and doubly protonated ion with a minimum intensity threshold of $7 \times 10^5$ ions.

**Isothermal titration calorimetry**

Purified recombinant proteins were dialyzed in degassed ITC (isothermal titration calorimetry) buffer. Peptides were dissolved directly in the dialysate. Titrations with Hck-SH3 and $ALIX_{V+PRR}$ were carried out in 10 mM Hepes (pH 7.5), 150 mM NaCl, 2 mM β-mercaptoethanol, and 2 mM EDTA. Hck-SH3 (at 600 µM) was injected from the syringe into the measurement cell containing $ALIX_{V+PRR}$ (at 50 µM). Titrations with Hck and PxxP peptides were performed in 10 mM Hepes (pH 7.5) and 150 mM NaCl; the peptides (at 3.8 mM) were injected into the cell containing Hck-SH3 (at 200 µM). All titrations were carried out at 25°C, using 10–15-µl injections. The concentration of the proteins prepared for ITC was measured with the NanoDrop 1000 spectrophotometer (Thermo Scientific). Data obtained from the injection of Hck-SH3 protein or peptide into 2 ml of ITC buffer were subtracted as blanks from the experimental data before the data were analyzed using Origin Software (OriginLab Corporation).

**NMR experiments**

To further elucidate the interaction mode between Hck-SH3 and $ALIX_{V+PRR}$ or PxxP peptides, $^{1}H$-$^{15}N$ HSQC (heteronuclear single quantum coherence) experiments were performed. Each H-N correlation peak is associated with the NH group of an amino acid. Mapping of the $ALIX_{V+PRR}$ or PxxP peptide interaction sites on Hck-SH3 was performed with a sample containing 50 µM uniformly $^{15}N$-labelled Hck-SH3 diluted in PBS buffer (50 µM $PO_4$ [pH 7.0], 150 µM NaCl, 5 mM DTT, and 2.5 mM EDTA) containing 10% $D_2O$. Titrations were performed by adding varying amounts of unlabeled $ALIX_{V+PRR}$ solution (1.45 mM) or PxxP peptide (3.3 mM) to varying final molar ratios of Hck-SH3:$ALIX_{V+PRR}$ (0.24–4.6) and Hck-SH3:PxxP peptide ( 0.40–10.2). At each step, a $^{1}H$-$^{15}N$ HSQC spectrum was recorded on a 600-MHz Bruker spectrometer (equipped with a CryoProbe). Heteronuclear assignments were taken from Horita et al. [26].

**Small-angle X-ray scattering (SAXS) data collection and analysis**

Data used for this SAXS (small angle X-ray scattering) analysis were collected at the SWING beamline of the SOLEIL synchrotron in Paris, France, at 10°C using a wavelength of $\lambda = 1.03$ Å. $ALIX_{V+PRR}$ at 20 mg/ml was applied to an HPLC-coupled size-exclusion column (Sephacryl S-200, Pharmacia), which outputs the fractions directly into the SAXS measuring cell. The HPLC run was performed in 50 mM Tris-HCl (pH 8.0), 150 mM NaCl, and 2 mM β-mercaptoethanol. Data on the fractions from the major peak were checked for consistent radius of gyration (using the Guinier approximation as implemented in the PRIMUS program) and pooled. Data were collected for a $q$ (scatter vector) range of 0.0066–0.6000 $Å^{-1}$. Data showing baseline absorbance at a wavelength of 280 nm were used as a buffer and subtracted from all collected data sets. Data analysis, *ab initio* shape calculations, and modelling of the flexible C-terminal regions (not included in the Alix V domain crystallographic structure of PDB (Protein Data Bank) entry 2OJQ [27]) were performed using the programs (PRIMUS, GNOM, DAMMIN, CRYSOL, DAMAVER, EOM, and BUNCH) of S. Svergun and colleagues (see the European Molecular Biology Laboratory website for more details: http://www.embl-hamburg.de/ExternalInfo/Research/Sax/software.html).

## RESULTS AND DISCUSSION

### Identification of Alix as a functional interactor of Hck

To search for and characterize novel downstream and/or regulatory binding partners of SFKs, we performed yeast two-hybrid screens using SH3 domains as bait; these identified Alix as a novel Hck SH3 domain interactor (experimental details to be published in S. Opi *et al.*; manuscript in preparation). Consistent with Hck-SH3 binding, the Alix C-terminal sequence contains a functional PRR already demonstrated by Schmidt *et al.* to be involved in GST–Src SH3 domain binding [20, 28]. The 'important' SH3-Src recognition sequence was indeed shown to be located in the $N_{term}$ region of the PRR (Pull-down experiments of Alix-P749A/P752A/P755A with the GST-Src SH3 domain pinpointed that mutation of the prolines in the Src-binding consensus sequence caused a reduction in the recovery of Alix, whereas mutation of proline residues outside of this region showed no effect). Unfortunately, the entire Cterminal region of Alix, comprising the PRR, could not be successfully purified and crystallized [17]. All together these published results make us decided to delete the very C-terminal residues until residue 760. To study and delineate more precisely the motif involved in Hck-SH3 binding and to optimize the conditions for expression and purification of the Alix PRR region, we developed two constructs (Figure 1). The first construct was designed to encode for the Alix V domain alone ($ALIX_V$, residues 362–702), and the second construct was designed to encode for the Alix V domain and the N-terminal part of the PRR region, with a stop codon at amino acid position 760 ($ALIX_{V+PRR}$, residues 362–760), thus conserving the SH3-binding motif defined by Schmidt *et al.* [20].

Both constructs encoded for recombinant proteins and could be produced and purified from bacteria cell cultures. Moreover, $ALIX_{V+PRR}$ was co-purified on a GST Hck-SH3 column, whereas the control GST affinity column alone did not retain the $ALIX_{V+PRR}$ recombinant protein (Figure 2A, lanes 2 and 3). We thus concluded that $ALIX_{V+PRR}$ and Hck-SH3 can interact *in vitro*. This $ALIX_{V+PRR}$–Hck-SH3 interaction was next confirmed in intact cells in a mammalian two-hybrid assay (previously described in Betzi *et al.* [24]). In this assay, the $ALIX_{V+PRR}$ construct was shown to induce transcription of the luciferase reporter gene upon co-expression with wild-type Hck-SH3 but not with a mutant, non functional Hck-SH3 (Figure 2B). To check whether this interaction is biologically relevant, we next verified that full-length Alix and Hck proteins can interact in mammalian cells. To do so, we co-transfected HEK-293 cells by a DNA construct encoding a Alix-GFP fusion protein and a DNA construct encoding the human Hck protein (Figure 2C). After anti-GFP immunoprecipitation of cell lysates and SDS-PAGE resolution, immunoblotting with anti-Hck antibodies revealed that Hck was specifically co-immunoprecipitated with the Alix-GFP fusion protein (upper panel, lane 3) but not with the GFP (upper panel, lane 1). Immunoblotting using anti-GFP antibodies verified similar immunoprecipitation levels of the Alix–GFP fusion protein (middle panel, lanes 2 and 3) and GFP (middle panel, lanes 1 and 4), and anti-Hck immunoblotting verified Hck expression levels (lower panel).

Once full-length Alix and Hck were shown to interact in mammalian cells the functional consequence of this Alix–Hck interaction was then investigated in an *in vitro* kinase assay. After co-expression of the full-length Alix and Hck proteins in HEK-293 cell cultures, Hck was

immunoprecipitated using specific anti-Hck antibodies, and its *ex cellulo* catalytic activity was determined. We compared the capability of cell-derived immunoprecipitated Hck to phosphorylate a polyglutamine-tyrosine peptide in the absence or presence of Alix-GFP (Figure 2D). As a positive control, Hck kinase activity was measured in the presence of HIV-1 Nef–GFP, an established Hck-SH3 ligand known to promote Hck activation [8]. Hck catalytic activity was found to increase upon co-expression with Alix or HIV-1 Nef, as indicated by increased $V_{max}$ (ATP) and decreased $K_m$ (ATP) values in the Michaelis–Menten plot (Figure 2D). We concluded that Hck not only interacted with Alix but also displayed a significantly increased catalytic activity upon co-expression with Alix in HEK-293 cells. Collectively, these results show that the Alix–Hck interaction is biologically relevant as the two proteins can interact structurally and functionally in mammalian cells.

**The PPII helix region of the Alix PRR interacts with the SH3 domain of Hck**

To evaluate the thermodynamic parameters of the interaction of $ALIX_{V+PRR}$ with the SH3 domain of Hck, we performed ITC experiments on the Hck-SH3–$ALIX_{V+PRR}$ association. The resulting ITC profile reflects a specific association between $Alix_{V+PRR}$ and Hck-SH3 (Figure 3A). From these measurements, we obtained an apparent equilibrium dissociation constant ($K_d$) of 34.5 µM and a stoichiometry of approximately 1:1 for the interaction between $ALIX_{V+PRR}$ and Hck-SH3. In addition, a nonporous silicon biosensor interferometry experiment validated the order of the $K_d$ value observed by ITC (Table 1 and Figure S1A). This deduced $K_d$ value is typical of the previously reported SH3–PPII helix peptide interaction ($K_d$ = 0.2–200 µM) [29]. We also used ITC to identify the residues of the $ALIX_{V+PRR}$ PxxP motif implicated in the interaction with Hck-SH3. Different proline-rich peptides from the $ALIX_{V+PRR}$ PRR were synthesized and were respectively named peptides PI (residues 737–760), PII (residues 748–760), and PIII (residues 737–746) (see Figure 1). These peptides were found to bind to Hck-SH3 (Figure 3B–D), yet PII and PIII failed to account for the full thermodynamic parameters displayed by $ALIX_{V+PRR}$ (Table 1). Indeed, the $K_d$ of PI, the longest peptide, is almost the same as that of $ALIX_{V+PRR}$, and the thermodynamic parameters of PI are similar to those of $ALIX_{V+PRR}$. PII, the minimum peptide, which possesses a canonical class II PxxPx(R/K) SH3 core binding motif, demonstrated a reduced affinity and significantly altered $\Delta H$ and $T\Delta S$ values compared with PI. Finally, PIII, that does not possess a canonical SH3-binding motif, could only demonstrate a weak affinity for Hck-SH3. These results pinpointed that the PII sequence interacts with Hck-SH3 as the PxxP core motif and that the PIII sequence complements this role to confer a higher specificity and affinity to this interaction. These results validate PI as the main sequence interacting with Hck-SH3. Interferometry experiments with nonporous silicon biosensors on the Hck-SH3–Alix peptide associations reproduced the same Kd trend as observed by ITC, although the interferometry $K_d$ values were higher than those from ITC (Table 1 and Figure S1B–D). The small thermodynamic differences that were found between PI and $ALIX_{V+PRR}$ might be explained by a more stable PPII-helix prestructuring of the SH3-binding region in the $ALIX_{V+PRR}$ construct. This is consistent with the more favorable $T\Delta S$ values observed for PI in the interaction with $ALIX_{V+PRR}$. Of course, we cannot exclude the possibility that additional contacts between regions outside PI and Hck-SH3 also contributed to the binding.

**The PPII helix/Hck-SH3 recognition involves non-canonical interactions**

To determine which SH3 residues were involved in the Hck-SH3–$ALIX_{V+PRR}$ interaction, we performed NMR HSQC experiments. The HSQC spectra in Figure 4 illustrate the binding interaction between Hck-SH3 and $ALIX_{V+PRR}$ or PI. The chemical shifts induced by $ALIX_{V+PRR}$ and PI on Hck-SH3 were measured by superimposing the HSQC spectra of Hck-SH3 in the free state onto the HSQC spectra of Hck-SH3 in the presence of different equivalents of $ALIX_{V+PRR}$ or PI (Figure 4A, B). The relative chemical shifts of Hck-SH3 in the presence of an almost saturating concentration of $ALIX_{V+PRR}$ (4.6 equivalents) or PI (10.2 equivalents) pinpointed that the two ligands affected almost the same residues on the Hck-SH3 surface (Figure 4C). Moreover, most of the residues involved in the interaction demonstrated similar shifts when $ALIX_{V+PRR}$ titration was compared with PI titration (which may be due to the comparability observed in $K_d$ values). The significantly affected residues are distributed in three regions: the RT loop, the nSrc loop, and the $3_{10}$ helix. A canonical PxxP interaction typically involves mainly the hydrophobic grooves formed by residues Tyr87, Glu113, Trp114, and Pro129 to Tyr132 (Figure 4D). The observed patch in the NMR experiment also involved amino acids of the RT loop, suggesting Hck-SH3-Alix interaction is non canonical.

Furthermore, the binding affinities of Hck-SH3 to $ALIX_{V+PRR}$ or PI were validated in NMR by measuring the chemical shifts of the residues within the observed interacting regions (data not shown). The deduced affinities were consistent with the results of our ITC and interferometry experiments (Kd of 52.2 ± 2.5 µM for the PI-Hck-SH3 complex and a Kd of 45.2± 4 µM for the $ALIX_{V+PRR}$-Hck-SH3 complex). The non-canonical recognition mode observed here was supported by previous studies of extended SH3 recognition sequences that implicated the nSrc loop and the RT loop in specific contacts with a non-canonical PxxP peptide [30, 31]. These additional interactions can enhance both affinity and selectivity for SH3 domains. A 3D structure or extensive biophysical and biochemical characterization will further elucidate the molecular details of this extended recognition mode.

**The PRR region of Alix is structurally unfolded and allows kinase recruitment**

Fisher *et al.* suggested that the PRR was disordered and that no structural details could be obtained regarding this highly disordered region [17]. To experimentally investigate the absence or presence of a folded SH3 recognition domain along $ALIX_{V+PRR}$ residues C-terminal to the V domain, we used SAXS technique. The SWING SAXS beamline used has a size-exclusion chromatography column directly feeding into the SAXS sample cell allowing on-line separation of the protein species prior to SAXS measurement. Size exclusion chromatography showed two significant peaks, consistent with previous data showing that V-domain-containing Alix recombinant proteins exist in a mixture of monomeric and dimeric forms [32]. Retention time and SDS-PAGE analysis are consistent with the major and minor peaks corresponding to monomeric and dimeric species, respectively (results not shown). Due to the lack of intensity of the presumed dimeric species, SAXS analysis could only be performed on the monomeric species. The *ab initio* envelopes calculated for this monomeric $ALIX_{V+PRR}$ protein suggested a model in which ALIX V domain is in its 'crystal structure' conformation (Figure S2). This monomeric conformation precedes the dimerization process of the protein, at least during HIV budding [32]. The envelope is also consistent with residues 703–760 of $ALIX_{V+PRR}$ protruding freely in the solvent without forming a folded domain and

without substantial contacts with the V domain. This finding was also supported by an analysis using the EOM (ensemble optimization method) program. EOM allows the selection of an ensemble of models that best fit the data, from an initially generated pool of about 10,000 randomly generated structures; we used the Alix V domain of PDB entry 2OJQ as the fixed structure and only varied the flexible residues 703–760. EOM-selected ensemble models showed a high flexibility and an extended structure of residues 703–760 (Figure 5).

## CONCLUSION

Our results support that Alix binds to and functionally activates Hck. The cellular roles of Alix overlap with those of Hck, contributing to regulation of cellular trafficking [33] and viral propagation [34]. Our analysis also identified amino acid residues 737–760 as an Alix proline-rich motif involved in Hck-SH3 domain binding. Alix was previously found to be an SH3-binding partner of endophilin, as evidenced by yeast two-hybrid analysis [11], and a functional binding partner of the SH2 and SH3 domains of the *Xenopus* and mammalian Src and Fyn orthologs [20, 35]. However, the molecular details of these interactions remained elusive. Here, we demonstrated that Alix residues outside of the canonical PxxP motif enhanced affinity and also possibly specificity for Hck-SH3. Future research should address whether this enlarged recognition motif is also used for targeting other SH3 domains or is selective for Hck-SH3.

Previous studies have demonstrated that the PR domain keeps Alix in an autoinhibited conformation [19]. Indeed, some flexibility degrees between the two arms of the V-shape domain could bring the N-terminal Bro 1 domain and C-terminal PR domain into spatial proximity allowing additional interactions between phosphotyrosine in patch 2 from the Bro1 domain and Src family SH2 domains. This proximity could then mediate an intra molecular interaction regulated by the PR domain, which would allowed to mask the binding sites in both Bro1 and V domain and thus inhibit the Alix activity. In presence of Src Kinase enzymes this conformational locked protein could then facilitate the Src kinase to interact with Bro1 and PR region simultaneously through its SH2 and SH3 domains, thus releasing the auto-inhibited Alix conformation into an open and active protein conformation. Our SAXS analysis supports this proposition since the observed structural flexibility of the PRR domain could enable it to mediate an intramolecular interaction inhibiting the activity of Alix and also to facilitate the interaction of Src kinase via its SH2 and SH3 domains with the Alix N-terminal Bro1 domain and C-terminal PRR domain, respectively. We therefore speculate that differences exist between the relative contributions of the SH2 and SH3 domains to the binding and that these might result in the functional differences of the complexes formed by Alix and Src kinases. The structural framework of the Hck–Alix interaction demonstrated here will help to elucidate how Hck and Alix assist in virus budding and regulation of cell surface receptors, which might be particularly relevant in monocytes and macrophages that specifically express Hck and that constitute an important reservoir for HIV spreading.

**ACKNOWLEDGMENTS**

The authors would like to thank Olivier Bornet for performing the NMR experiments, Marielle Beauzan for bacterial expression, Karen Muller for editorial assistance, and Dieter Vermeire for Biacore support. We thank the SOLEIL synchrotron source in Paris, France, for SAXS beam time. The HPLC in line with the SAXS sample cell was developed with support from the European grant SAXIER: EU FP6 Design study SAXIER, grant number RIDS 011934. The project was supported by the CNRS, INSERM, ANRS (Agence Nationale de Recherche sur le SIDA et les hépatites virales), MOST (2007CB914304 and 2006AA02A313), NSFC (30800181 and 30625011), the FWO and the concerted action program of the Katholieke Universiteit Leuven. S.O. and A.L. were fellows of the ANRS, and X.S. was a fellow of the 'Ambassade de France en Chine'. This research is supported in part by the National Institutes of Health through MD Anderson's Cancer Center Support Grant CA016672. JC acknowledges the support of the Canada Research Chair in Medical Genomics

**SUPPLEMENTARY DATA**

Supplementary data are available for the interferometry experiments (Supplementary Figure S1) and for SAXS analysis (Supplementary Figure S2).

## REFERENCES


1 Thomas, S. and Brugge, J. (1997) Cellular functions regulated by Src family kinases. Annu. Rev. Cell Dev. Biol. **13**, 513-609

2 Parsons, S. and Parsons, J. (2004) Src family kinases, key regulators of signal transduction. Oncogene **23**, 7906-7909

3 Yeatman, T. (2004) A renaissance for SRC. Nat. Rev. Cancer **4**, 470-480

4 Collette, Y. and Olive, D. (1997) Non-receptor protein tyrosine kinases as immune targets of viruses. Immunol. Today **18**, 393-400

5 Sicheri, F., Moarefi, I. and Kuriyan, J. (1997) Crystal structure of the Src family tyrosine kinase Hck. Nature **385**, 602-609

6 Xu, W., Harrison, S. and Eck, M. (1997) Three-dimensional structure of the tyrosine kinase c-Src. Nature **385**, 595-602

7 Matsuda, M., Mayer, B., Fukui, Y. and Hanafusa, H. (1990) Binding of transforming protein, P47gag-crk, to a broad range of phosphotyrosine-containing proteins. Science **248**, 1537-1539

8 Moarefi, I., LaFevre-Bernt, M., Sicheri, F., Huse, M., Lee, C., Kuriyan, J. and Miller, W. (1997) Activation of the Src-family tyrosine kinase Hck by SH3 domain displacement. Nature **385**, 650-653

9 Superti-Furga, G., Fumagalli, S., Koegl, M., Courtneidge, S. and Draetta, G. (1993) Csk inhibition of c-Src activity requires both the SH2 and SH3 domains of Src. EMBO J. **12**, 2625-2634

10 Superti-Furga, G. and Courtneidge, S. (1995) Structure-function relationships in Src family and related protein tyrosine kinases. Bioessays **17**, 321-330

11 Chatellard-Causse, C., Blot, B., Cristina, N., Torch, S., Missotten, M. and Sadoul, R. (2002) Alix (ALG-2-interacting protein X), a protein involved in apoptosis, binds to endophilins and induces cytoplasmic vacuolization. J. Biol. Chem. **277**, 29108-29115

12 Katoh, K., Shibata, H., Suzuki, H., Nara, A., Ishidoh, K., Kominami, E., Yoshimori, T. and Maki, M. (2003) The ALG-2-interacting protein Alix associates with CHMP4b, a human homologue of yeast Snf7 that is involved in multivesicular body sorting. J. Biol. Chem. **278**, 39104-39113

13 Kurakin, A., Wu, S. and Bredesen, D. (2003) Atypical recognition consensus of CIN85/SETA/Ruk SH3 domains revealed by target-assisted iterative screening. J. Biol. Chem. **278**, 34102-34109

14 Matsuo, H., Chevallier, J., Mayran, N., Le Blanc, I., Ferguson, C., Fauré, J., Blanc, N., Matile, S., Dubochet, J., Sadoul, R., Parton, R., Vilbois, F. and Gruenberg, J. (2004) Role of LBPA and Alix in multivesicular liposome formation and endosome organization. Science **303**, 531-534

15 Strack, B., Calistri, A., Craig, S., Popova, E. and Göttlinger, H. (2003) AIP1/ALIX is a binding partner for HIV-1 p6 and EIAV p9 functioning in virus budding. Cell **114**, 689-699

16 Trioulier, Y., Torch, S., Blot, B., Cristina, N., Chatellard-Causse, C., Verna, J. and Sadoul, R. (2004) Alix, a protein regulating endosomal trafficking, is involved in neuronal death. J. Biol. Chem. **279**, 2046-2052

17 Fisher, R., Chung, H., Zhai, Q., Robinson, H., Sundquist, W. and Hill, C. (2007) Structural

and biochemical studies of ALIX/AIP1 and its role in retrovirus budding. Cell **128**, 841-852
18 Zhai, Q., Fisher, R., Chung, H., Myszka, D., Sundquist, W. and Hill, C. (2008) Structural and functional studies of ALIX interactions with YPX(n)L late domains of HIV-1 and EIAV. Nat. Struct. Mol. Biol. **15**, 43-49
19 Zhou, X., Pan, S., Sun, L., Corvera, J., Lee, Y., Lin, S. and Kuang, J. (2009) The CHMP4b- and Src-docking sites in the Bro1 domain are autoinhibited in the native state of Alix. Biochem. J. **418**, 277-284
20 Schmidt, M., Dikic, I. and Bögler, O. (2005) Src phosphorylation of Alix/AIP1 modulates its interaction with binding partners and antagonizes its activities. J. Biol. Chem. **280**, 3414-3425
21 Picard, C., Greenway, A., Holloway, G., Olive, D. and Collette, Y. (2002) Interaction with simian Hck tyrosine kinase reveals convergent evolution of the Nef protein from simian and human immunodeficiency viruses despite differential molecular surface usage. Virology **295**, 320-327
22 Marblestone, J. G., Edavettal, S. C., Lim, Y., Lim, P., Zuo, X. and Butt, T. R. (2006) Comparison of SUMO fusion technology with traditional gene fusion systems: enhanced expression and solubility with SUMO. Protein Sci. **15**, 182-189
23 Weeks, S. D., Drinker, M. and Loll, P. J. (2007) Ligation independent cloning vectors for expression of SUMO fusions. Protein Expr. Purif. **53**, 40-50
24 Betzi, S., Restouin, A., Opi, S., Arold, S., Parrot, I., Guerlesquin, F., Morelli, X. and Collette, Y. (2007) Protein protein interaction inhibition (2P2I) combining high throughput and virtual screening: Application to the HIV-1 Nef protein. Proc. Natl. Acad. Sci. U.S.A. **104**, 19256-19261
25 Arold, S., Franken, P., Strub, M., Hoh, F., Benichou, S., Benarous, R. and Dumas, C. (1997) The crystal structure of HIV-1 Nef protein bound to the Fyn kinase SH3 domain suggests a role for this complex in altered T cell receptor signaling. Structure **5**, 1361-1372
26 Horita, D., Baldisseri, D., Zhang, W., Altieri, A., Smithgall, T., Gmeiner, W. and Byrd, R. (1998) Solution structure of the human Hck SH3 domain and identification of its ligand binding site. J. Mol. Biol. **278**, 253-265
27 Lee, S., Joshi, A., Nagashima, K., Freed, E. and Hurley, J. (2007) Structural basis for viral late-domain binding to Alix. Nat. Struct. Mol. Biol. **14**, 194-199
28 Dejournett, R., Kobayashi, R., Pan, S., Wu, C., Etkin, L., Clark, R., Bögler, O. and Kuang, J. (2007) Phosphorylation of the proline-rich domain of Xp95 modulates Xp95 interaction with partner proteins. Biochem. J. **401**, 521-531
29 Ladbury, J. and Arold, S. (2000) Searching for specificity in SH domains. Chem. Biol. **7**, R3-8
30 Santiveri, C., Borroto, A., Simón, L., Rico, M., Alarcón, B. and Jiménez, M. (2009) Interaction between the N-terminal SH3 domain of Nck-alpha and CD3-epsilon-derived peptides: non-canonical and canonical recognition motifs. Biochim. Biophys. Acta **1794**, 110-117
31 Schmidt, H., Hoffmann, S., Tran, T., Stoldt, M., Stangler, T., Wiesehan, K. and Willbold, D. (2007) Solution structure of a Hck SH3 domain ligand complex reveals novel interaction modes. J. Mol. Biol. **365**, 1517-1532
32 Pires, R., Hartlieb, B., Signor, L., Schoehn, G., Lata, S., Roessle, M., Moriscot, C., Popov,

S., Hinz, A., Jamin, M., Boyer, V., Sadoul, R., Forest, E., Svergun, D., Göttlinger, H. and Weissenhorn, W. (2009) A crescent-shaped ALIX dimer targets ESCRT-III CHMP4 filaments. Structure **17**, 843-856

33 Guiet, R., Poincloux, R., Castandet, J., Marois, L., Labrousse, A., Le Cabec, V. and Maridonneau-Parini, I. (2008) Hematopoietic cell kinase (Hck) isoforms and phagocyte duties - from signaling and actin reorganization to migration and phagocytosis. Eur. J. Cell Biol. **87**, 527-542

34 Hassaïne, G., Courcoul, M., Bessou, G., Barthalay, Y., Picard, C., Olive, D., Collette, Y., Vigne, R. and Decroly, E. (2001) The tyrosine kinase Hck is an inhibitor of HIV-1 replication counteracted by the viral vif protein. J. Biol. Chem. **276**, 16885-16893

35 Che, S., El-Hodiri, H., Wu, C., Nelman-Gonzalez, M., Weil, M., Etkin, L., Clark, R. and Kuang, J. (1999) Identification and cloning of xp95, a putative signal transduction protein in Xenopus oocytes. J. Biol. Chem. **274**, 5522-5531

36 Grzesiek, S., Bax, A., Clore, G., Gronenborn, A., Hu, J., Kaufman, J., Palmer, I., Stahl, S. and Wingfield, P. (1996) The solution structure of HIV-1 Nef reveals an unexpected fold and permits delineation of the binding surface for the SH3 domain of Hck tyrosine protein kinase. Nat. Struct. Biol. **3**, 340-345

## FIGURE LEGENDS

**Figure 1. Alix constructs and peptides**
The Bro1 and V domains of Alix are shown in dark and grey, respectively. The different Alix constructs and peptides used in this study are depicted schematically. The PxxP region is highlighted in bold.

**Figure 2. Alix interacts with Hck and regulates Hck kinase activity**
(A) Purified Alix ($ALIX_{V+PRR}$; amino acids 362–760) was incubated at room temperature for 2 h with Sepharose-coupled recombinant GST (lane 2) or GST Hck-SH3 (lane 3) under agitation. After column purification and extensive washing, the resulting protein complexes were resolved by 12% SDS-PAGE and stained with Coomassie Blue. As control, $ALIX_{V+PRR}$ was loaded in lane 1. (B) COS7 cells were co-transfected with VP16–$ALIX_{V+PRR}$, GAL4–Hck-SH3 (wild-type or mutant), and a GAL4–Luc construct encoding for the firefly luciferase reporter gene. Cells were lysed 36 h after transfection, and luciferase levels were determined. Results for the ratio of firefly (FF) to *Renilla* (RN) luciferase are presented as normalized values, as described in the Experimental section. (C) HEK-293 cells were co-transfected with Hck and Alix–GFP or GFP plasmid constructs. Cells were harvested 24 h after transfection, and cell lysates were subjected to immunoprecipitation using anti-GFP antibodies followed by immunoblotting using the indicated antibodies. (D) HEK-293 cells were co-transfected with Hck and Alix–GFP, HIV-1 Nef–GFP, or GFP plasmid constructs. Cells were harvested 24 h after transfection, and cell lysates were immunoprecipitated using Hck-specific polyclonal antibodies. Immune complexes were washed twice and incubated for 30 min at 30°C with varying amounts of ATP (0–10 mM) on a 96-well MaxiSorp plate previously coated with polyglutamine-tyrosine peptide. The fraction of phosphorylated substrate was visualized using a phosphotyrosine monoclonal antibody conjugated to HRP and an ensuing chromogenic substrate reaction.

**Figure 3. Characterization of Hck-SH3 binding to $ALIX_{V+PRR}$ and Alix PxxP peptides by ITC**
Experimental ITC binding curves for the interaction of Hck-SH3 with (A) $ALIX_{V+PRR}$, (B) PI, (C) PII, and (D) PIII. Top panel illustrates the raw ITC data obtained from an experiment. Bottom panel illustrates the nonlinear least squares fit to the data from the top panel after blank subtraction, for each complex.

**Figure 4. Mapping of the atomic recognition surface by heteronuclear NMR**
(A, B) $^{1}H$-$^{15}N$ NMR HSQC spectra of $^{15}N$-labeled Hck-SH3 in the presence of an increasing concentration of unlabeled $ALIX_{V+PRR}$ (A) and PI (B). The HSQC spectra at 0, 1, 2.5, 5, and 10.2 equivalents of ligands are shown in black, pink, green, red, and blue, respectively. (C) The relative chemical shifts of Hck-SH3 residues observed in the presence of 4.6 equivalents of $ALIX_{V+PRR}$ and 10.2 equivalents of PI are shown in dark and light gray, respectively. The relative variations of $^{1}H$ and $^{15}N$ were calculated according to Grzesiek et al. [36] (D) Corresponding chemical shift mapping on the surface of Hck-SH3 (PDB code: 1BU1) in the

presence of $ALIX_{V+PRR}$ and PI. Small chemical shift changes are shaded in yellow, larger shifts are in orange, and the largest shifts are in red.

**Figure 5. SAXS model of $ALIX_{V+PRR}$**

(A) Fit of EOM SAXS ensemble model (grey) to data (black). (B) Three representative structural models produced by EOM based on SAXS data were superimposed on their Alix V domain, displayed as a light grey ribbon (PDB code: 2OJQ). Pseudo residues placed by EOM (spheres) are grayed differently for each individual model.

Biochemical Journal Immediate Publication. Published on 29 Jul 2010 as manuscript BJ20100314



| | | | $Alix_{V+PRR}$ | PI | PII | PIII |
|---|---|---|---|---|---|---|
| **ITC** | **n** | | 0.80 +/- 0.2 | 1.28 +/- 0.3 | 1.22 +/- 0.2 | 1.24 +/- 0.3 |
| | **$K_d$** | *(µM)* | **34.5 +/- 3.3** | **30.9 +/- 3.2** | **42.2 +/- 2.1** | **142 +/- 6.2** |
| | **ΔH** | *(KJ/mol)* | -15.1 +/- 1.2 | -19.3 +/- 0.4 | -26.5 +/- 0.4 | -26.8 +/- 0.7 |
| | **TΔS** | *(KJ/mol)* | 10.4 | 6.5 | -1.6 | -4.8 |
| | **ΔG** | *(KJ/mol)* | -25.5 | -25.8 | -24.9 | -22.0 |
| | | | | | | |
| **Interferometry** | **$K_d$** | *(µM)* | **45.3** | **79.4** | **169.7** | **>1000** |
| | **$X^2$** | | 3 $e^{-2}$ | 1.1 $e^{-3}$ | 9.7$e^{-4}$ | N/D |

**Table 1:** Binding constants of Hck-SH3 to $Alix_{V+PRR}$ or ALIX derived PxxP peptides**.**
***n**: stoichiometry, **$K_d$** : binding constant, **$X^2$**: curve fit*

Biochemical Journal Immediate Publication. Published on 29 Jul 2010 as manuscript BJ20100314



**Figure 1**

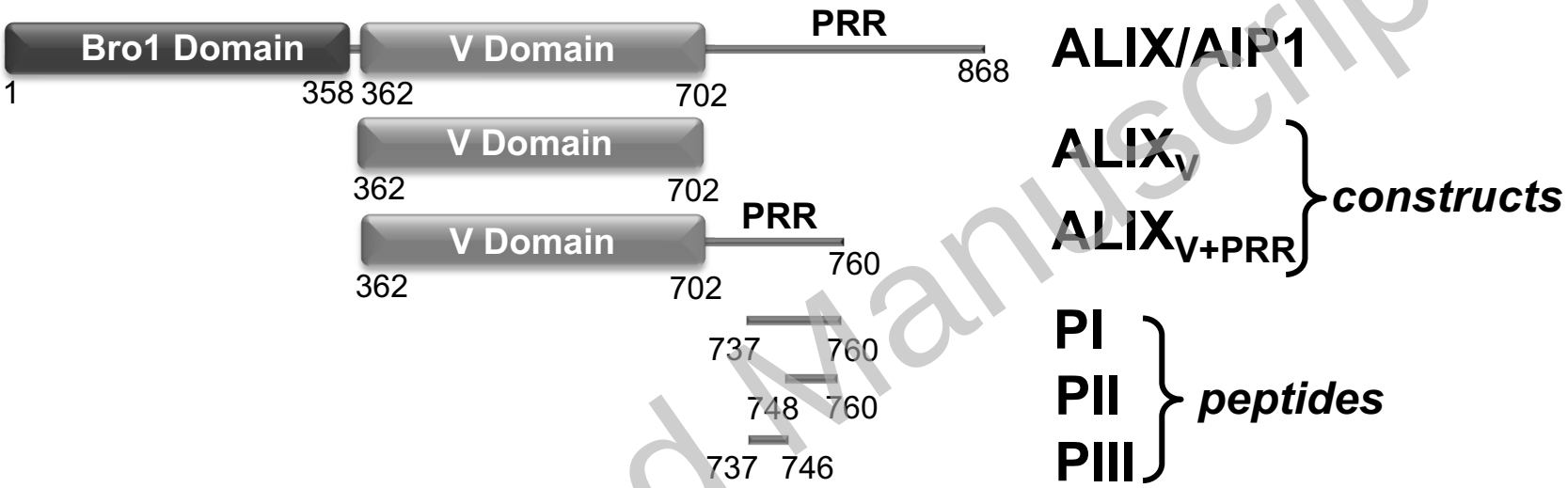


**Alix peptide PI**: $_{737}$PTPPTPAPRTMPPTK**PQPPAR**PPP$_{760}$

**Alix peptide PII**: $_{748}$PPTK**PQPPAR**PPP$_{760}$

**Alix peptide PIII**: $_{737}$PTPPTPAPRT$_{746}$

Biochemical Journal Immediate Publication. Published on 29 Jul 2010 as manuscript BJ20100314



# Figure 2

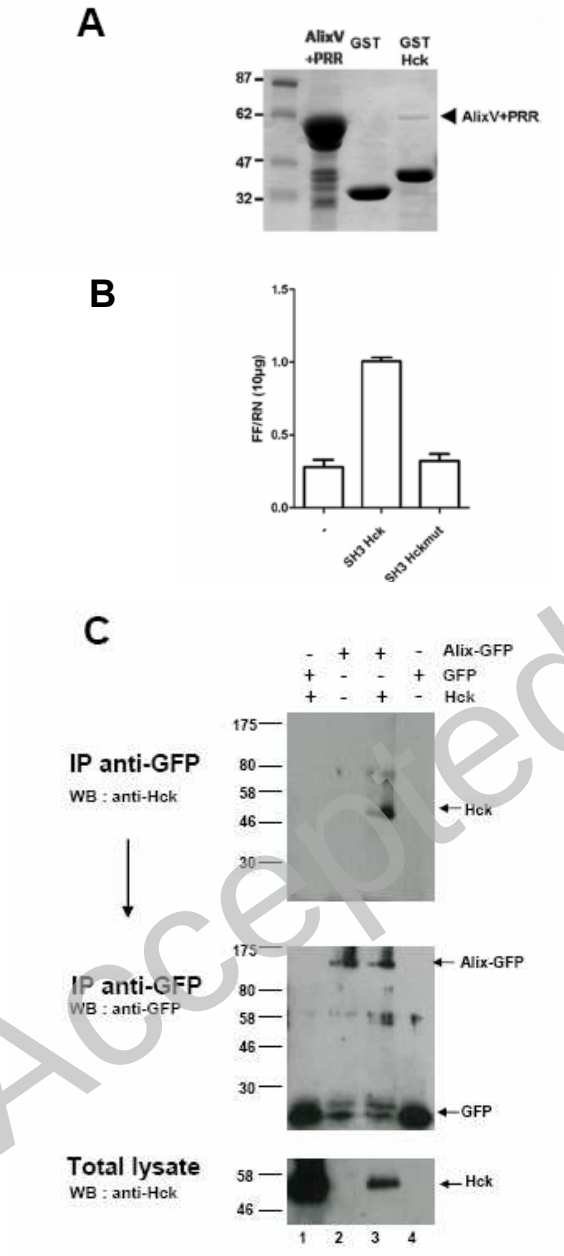


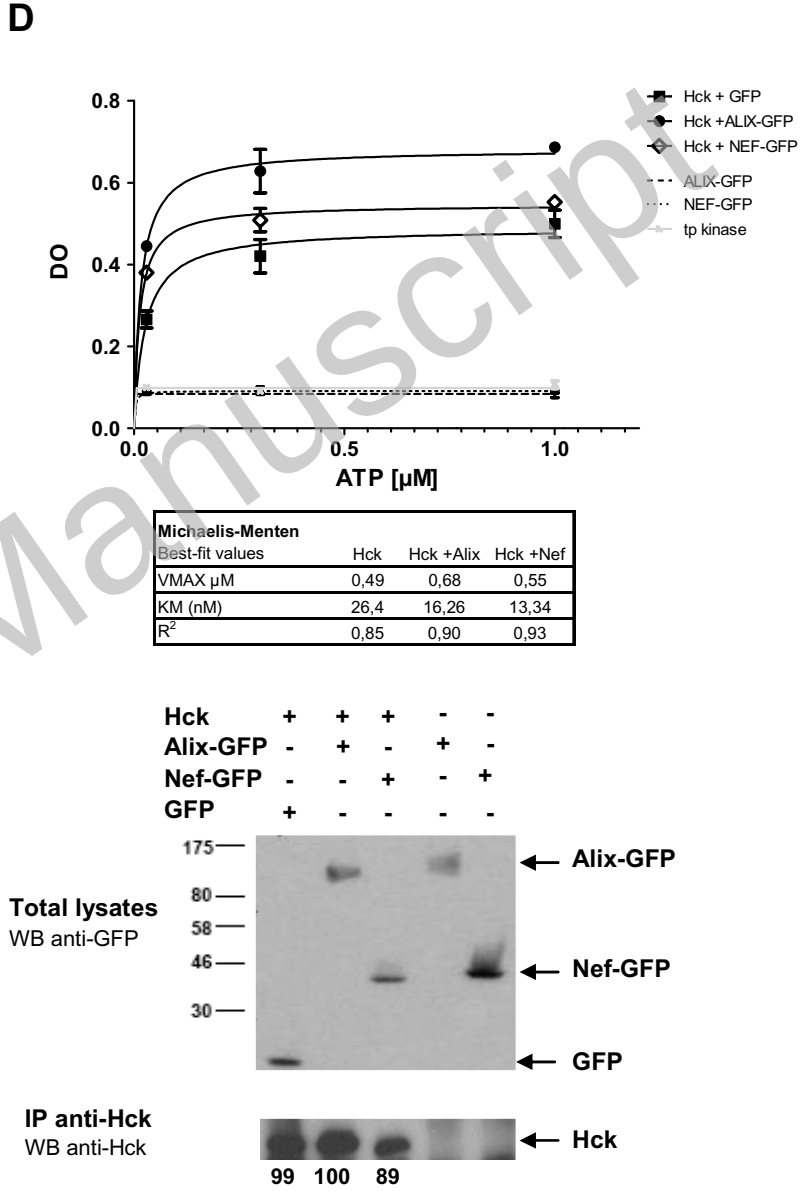


**Michaelis-Menten**

| Best-fit values | Hck | Hck +Alix | Hck +Nef |
|---|---|---|---|
| VMAX µM | 0,49 | 0,68 | 0,55 |
| KM (nM) | 26,4 | 16,26 | 13,34 |
| $R^2$ | 0,85 | 0,90 | 0,93 |

# Figure 3

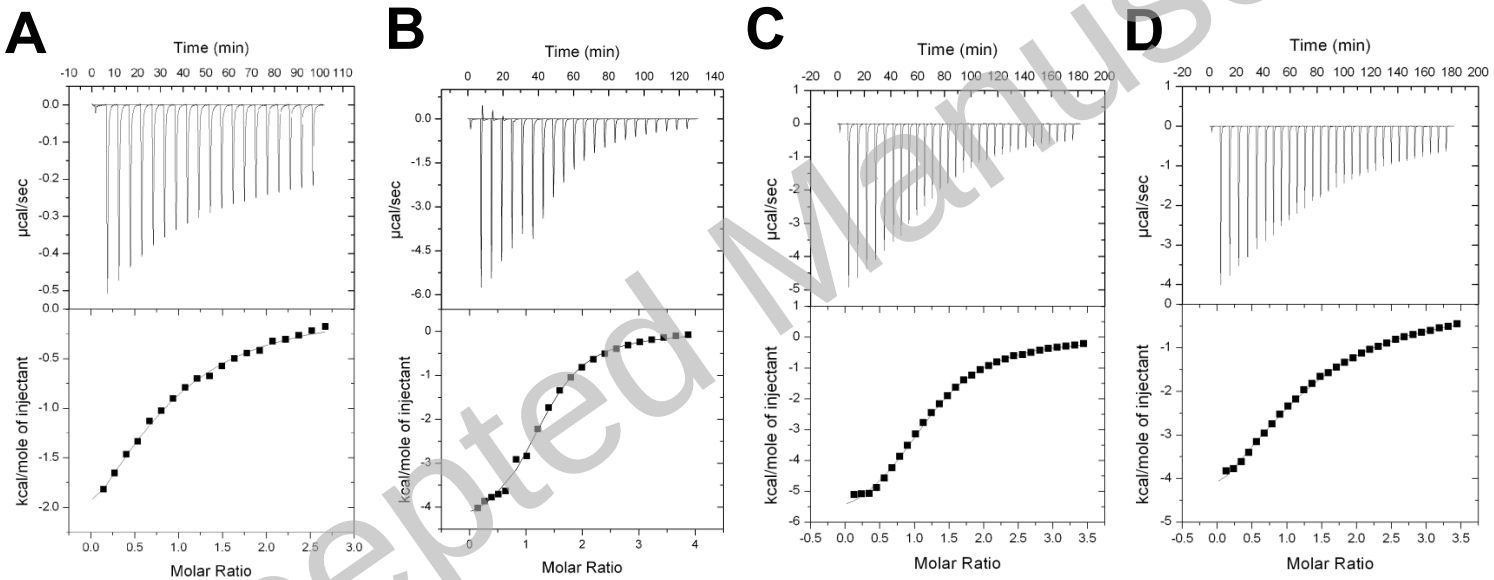

Biochemical Journal Immediate Publication. Published on 29 Jul 2010 as manuscript BJ20100314



**Figure 4**

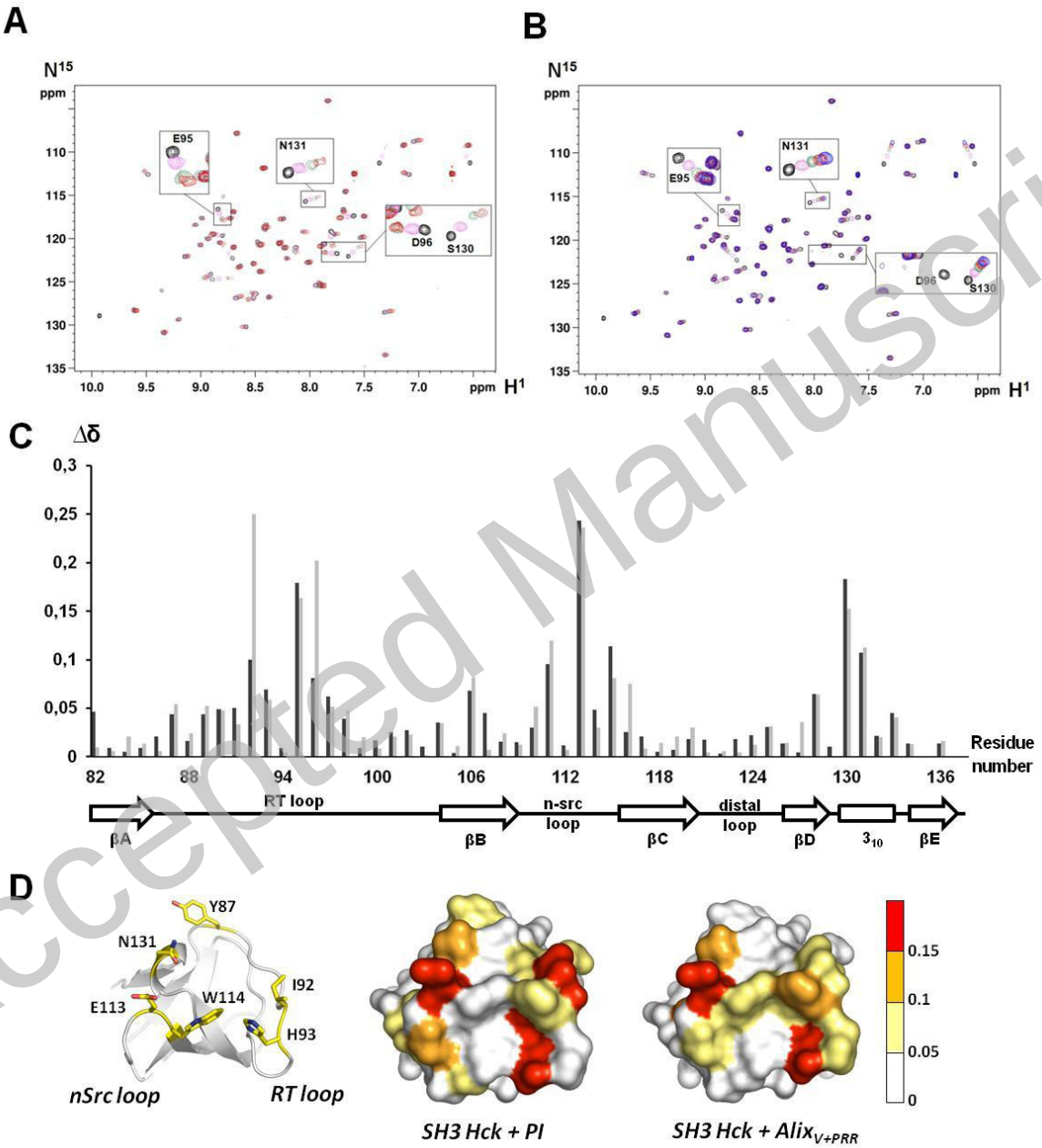

Biochemical Journal Immediate Publication. Published on 29 Jul 2010 as manuscript BJ20100314



**Figure 5**